Sectioned Warp Shell Dynamics: Field Equations and Control Topology for Warp Sections/Antisections with an SFG Toroidal Lattice

Hrishi Mukherjee

Simulonic Research Notes

Abstract

We extend a sectioned ellipsoidal warp-shell depiction into a formal set of field equations and a control topology. The shell is partitioned into warp sections and warp antisections, modeled as phase-opposed modal domains of a scalar warp potential and an associated flux field. A toroidal ring of twelve Simulonic Field Generators (SFGs) is treated as a discrete, phase-locked actuator lattice that couples opposed antisections through controlled phase exchange. The Harmonic Oscillator (HO) provides a global phase/time reference; the Inertial Null Core (INC) imposes an inertial-gradient sink condition. We provide (i) a PDE model for the shell potential with section/antisection source terms, (ii) a discrete coupling law on the SFG ring, and (iii) a closed-loop control architecture consistent with the four schematic depictions.

Keywords: Warp Sections, Warp Antisections, SFG Lattice, Phase Exchange, HO Reference, INC Sink, Control Topology

1. Geometric Preliminaries and Partitioning

Let the craft axis be $\hat{\mathbf{x}}$ and let the warp shell be an ellipsoidal surface with interior $\Omega \subset \mathbb{R}^3$ and boundary $\partial\Omega$. We define a partition of the shell into four *sections* and four *antisections*:

$$\partial\Omega = \left(\bigcup_{j=1}^{4} \Sigma_j\right) \cup \left(\bigcup_{\ell=1}^{4} \bar{\Sigma}_\ell\right), \qquad \Sigma_j \cap \bar{\Sigma}_\ell = \emptyset.$$

Define indicator functions (or smooth masks) on $\partial\Omega$:

$$\chi_{\Sigma_j}(\mathbf{x}) = \begin{cases} 1, & \mathbf{x} \in \Sigma_j \\ 0, & \text{else} \end{cases}, \qquad \chi_{\bar{\Sigma}_\ell}(\mathbf{x}) = \begin{cases} 1, & \mathbf{x} \in \bar{\Sigma}_\ell \\ 0, & \text{else.} \end{cases}$$

In implementations, replace these with smooth window functions to avoid sharp discontinuities.

2. Section/Antisection Field Variables

2.1. Warp potential and flux

Introduce a scalar warp potential $\Phi(\mathbf{x}, t)$ on Ω and its associated flux-like field

$$\boxed{\mathbf{J}(\mathbf{x}, t) := -\kappa \nabla\Phi(\mathbf{x}, t)} \tag{1}$$

where $\kappa > 0$ is an effective stiffness/coupling constant. (This is the minimal gradient-flow form; tensor generalizations are allowed.)

2.2. Phase-opposed decomposition

Define the shell potential as a signed sum of *section* and *antisection* contributions:

$$\boxed{\Phi(\mathbf{x}, t) = \sum_{j=1}^{4} \Phi_j^{(+)}(\mathbf{x}, t) \; - \; \sum_{\ell=1}^{4} \Phi_\ell^{(-)}(\mathbf{x}, t)} \tag{2}$$

where (+) denotes constructive curvature domains (sections) and (−) denotes counter-curvature domains (antisections).

A compact boundary representation uses section/antisection amplitudes $a_j(t)$ and $\bar{a}_\ell(t)$:

$$\boxed{\Phi\big|_{\partial\Omega}(\mathbf{x}, t) = \sum_{j=1}^{4} a_j(t)\, \psi_j(\mathbf{x}) - \sum_{\ell=1}^{4} \bar{a}_\ell(t)\, \bar{\psi}_\ell(\mathbf{x})} \tag{3}$$

where $\psi_j, \bar{\psi}_\ell$ are boundary shape functions supported primarily on Σ_j and $\bar{\Sigma}_\ell$ (e.g., windowed spherical harmonics or localized ellipsoidal patches).

3. PDE Model for the Warp Shell Potential

We model Φ as a damped, screened field driven by (i) SFG lattice sources, (ii) MEA boundary actuation, and (iii) HO/INC constraints.

3.1. Interior dynamics (screened wave / diffusion-wave)

A flexible form that covers quasi-static and dynamic regimes is:

$$\boxed{\partial_{tt}\Phi + 2\zeta\omega_0\, \partial_t\Phi = c_\Phi^2\, \nabla^2\Phi - \omega_0^2\, \Phi + S_{\text{SFG}}(\mathbf{x}, t)} \tag{4}$$

Parameters:

- c_Φ : effective propagation speed of warp potential updates,
- ω_0 : screening (sets characteristic shell thickness / confinement),
- ζ : damping ratio (stability knob),

- S_{SFG} : discrete actuation injected by the SFGs (defined next).

Quasi-static limit (if desired): set $\partial_{tt}\Phi \approx 0$, $\partial_t\Phi \approx 0$ to obtain

$$(c_\Phi^2\nabla^2 - \omega_0^2)\Phi + S_{\mathrm{SFG}} \approx 0.$$

3.2. Discrete SFG actuation as localized sources

Let there be $N = 12$ SFGs located on the toroidal ring at positions $\{\mathbf{p}_k\}_{k=0}^{11}$. Model their injection into the field as:

$$\boxed{S_{\mathrm{SFG}}(\mathbf{x},t) = \sum_{k=0}^{11} u_k(t)\, G_\sigma(\mathbf{x}-\mathbf{p}_k)} \tag{5}$$

where $u_k(t)$ is the commanded actuation (complex or real amplitude) and

$$G_\sigma(\mathbf{r}) = \exp\!\left(-\frac{\|\mathbf{r}\|^2}{2\sigma^2}\right)$$

is a compact kernel (replace with a delta distribution in idealized theory).

3.3. MEA boundary actuation as Neumann/Robin control

Model the MEA strips as boundary-condition control regions $\Gamma_A, \Gamma_P \subset \partial\Omega$. A standard controlled Robin boundary law is:

$$\boxed{\alpha\,\Phi + \beta\,\partial_n\Phi = b_{\mathrm{MEA}}(\mathbf{x},t), \qquad \mathbf{x}\in\Gamma_A\cup\Gamma_P} \tag{6}$$

where ∂_n is the outward normal derivative and b_{MEA} is driven by MEA commands (continuous smoothing / damping control).

4. HO Reference and INC Sink Constraints

4.1. HO as global phase/time reference

Let the HO provide a reference oscillator:

$$\boxed{r_{\mathrm{HO}}(t) = A_{\mathrm{HO}}\cos(\omega_{\mathrm{HO}}t + \phi_0)} \tag{7}$$

and define a global phase variable $\theta(t)$ tracked by the control system:

$$\theta(t) = \omega_{\mathrm{HO}}t + \phi_0.$$

Each SFG command is phase-locked to $\theta(t)$:

$$\boxed{u_k(t) = \mathrm{Re}\left\{\, U_k(t)\, e^{i\theta(t)}\right\}} \tag{8}$$

where $U_k(t)$ is a slowly varying complex envelope controlled for shaping.

4.2. INC as inertial-gradient sink condition

Model the INC as enforcing a local "gradient sink" near its location $\mathbf{p}_{\mathrm{INC}}$:

$$\boxed{\nabla\Phi(\mathbf{x},t) \to \mathbf{0} \quad \text{as} \quad \mathbf{x}\to\mathbf{p}_{\mathrm{INC}}} \tag{9}$$

Operationally, implement this as an interior penalty term on a small INC region Ω_{INC}:

$$\boxed{\partial_{tt}\Phi + 2\zeta\omega_0\,\partial_t\Phi = c_\Phi^2\nabla^2\Phi - \omega_0^2\Phi + S_{\mathrm{SFG}} - \eta_{\mathrm{INC}}\,\chi_{\Omega_{\mathrm{INC}}}\,\nabla^2\Phi} \tag{10}$$

where $\eta_{\mathrm{INC}} > 0$ increases smoothing/flattening near the INC, suppressing recoil-like gradients.

5. Section/Antisection Coupling via an SFG Phase-Exchange Law

Your schematics suggest that *opposing antisections* are coupled through the ring. We formalize that by defining antisection amplitudes $\bar{a}_\ell(t)$ and enforcing a controlled exchange current between opposite pairs.

5.1. Antisection pairing

Define an "opposition map" $\pi(\ell)$ over antisections:

$$\pi(1) = 3, \quad \pi(3) = 1, \qquad \pi(2) = 4, \quad \pi(4) = 2,$$

matching the visual i↔iii and ii↔iv pairing.

5.2. Exchange dynamics on antisection amplitudes

Let $\bar{\mathbf{a}}(t) = [\bar{a}_1, \bar{a}_2, \bar{a}_3, \bar{a}_4]^\top$. Define exchange currents $q_\ell(t)$ from ℓ to $\pi(\ell)$:

$$\boxed{\dot{\bar{a}}_\ell(t) = -\gamma\,\bar{a}_\ell(t) + \sum_{m=1}^{4} \mathsf{C}_{\ell m}\, q_m(t)} \tag{11}$$

where $\gamma > 0$ is damping and C is a signed incidence matrix encoding directionality. A minimal choice:

$$q_\ell(t) = k_\ell\left(\bar{a}_{\pi(\ell)}(t) - \bar{a}_\ell(t)\right).$$

This yields:

$$\boxed{\dot{\bar{a}}_\ell = -\gamma\,\bar{a}_\ell + k_\ell\left(\bar{a}_{\pi(\ell)} - \bar{a}_\ell\right)} \tag{12}$$

so opposed antisections relax toward balance while being damped.

5.3. How the SFG ring implements $q_\ell(t)$

Partition the 12 SFGs into four groups of three, one group per antisection:

$$\mathcal{K}_\ell \subset \{0,\dots,11\}, \qquad |\mathcal{K}_\ell| = 3, \qquad \bigcup_{\ell=1}^{4}\mathcal{K}_\ell = \{0,\dots,11\}.$$

Define group envelopes:

$$U_\ell(t) = \frac{1}{|\mathcal{K}_\ell|}\sum_{k\in\mathcal{K}_\ell} U_k(t).$$

Impose that exchange current is proportional to *relative phase-biased amplitude* between opposed groups:

$$\boxed{q_\ell(t) = \mu\ \mathrm{Im}\left\{U_\ell(t)\,\overline{U_{\pi(\ell)}(t)}\right\}} \tag{13}$$

so phase relations across opposed antisections drive exchange, consistent with the "criss-cross" coupling paths in your third depiction.

6. Closed-Loop Control Topology

We now provide the control architecture connecting HO, SFG ring, MEAs, and INC constraint. The structure is: HO sets reference phase; a controller computes desired section/antisection amplitudes; a mixer maps these to SFG/MEA commands; sensors estimate shell state; INC imposes sink constraint.

6.1. State, references, and errors

Define a reduced shell state vector:

$$\mathbf{x}_s(t) = \begin{bmatrix} \mathbf{a}(t) \\ \bar{\mathbf{a}}(t) \\ \dot{\mathbf{a}}(t) \\ \dot{\bar{\mathbf{a}}}(t) \end{bmatrix}, \quad \mathbf{a}(t) = [a_1, a_2, a_3, a_4]^\top, \quad \bar{\mathbf{a}}(t) = [\bar{a}_1, \bar{a}_2, \bar{a}_3, \bar{a}_4]^\top.$$

Let $\mathbf{x}_s^\star(t)$ be the desired setpoints (bubble shape + stability). Error:

$$\mathbf{e}(t) = \mathbf{x}_s^\star(t) - \mathbf{x}_s(t).$$

6.2. Controller and actuator mapping

A generic stabilizing control law:

$$\boxed{\mathbf{v}(t) = \mathsf{K}_P\, \mathbf{e}(t) + \mathsf{K}_D\, \dot{\mathbf{e}}(t)} \tag{14}$$

where $\mathbf{v}(t)$ encodes desired modal drive for sections/antisections.

Map $\mathbf{v}$ to SFG envelopes $\mathbf{U} = [U_0, \ldots, U_{11}]^\top$ with a mixing matrix M:

$$\boxed{\mathbf{U}(t) = \mathsf{M}\, \mathbf{v}(t)} \tag{15}$$

and then to real actuation via HO phase-lock:

$$u_k(t) = \mathrm{Re}\{U_k(t) e^{i\theta(t)}\}.$$

MEA boundary commands are computed as a smoothing/damping action on shell error:

$$\boxed{b_{\mathrm{MEA}}(\mathbf{x}, t) = -\lambda_{\mathrm{MEA}}\, \Phi(\mathbf{x}, t) - \nu_{\mathrm{MEA}}\, \partial_t \Phi(\mathbf{x}, t), \quad \mathbf{x} \in \Gamma_A \cup \Gamma_P.} \tag{16}$$

6.3. Topology diagram (block schematic)

7. Practical Reading of the Four Depictions (Now with Math)

Sections/Antisections as modal masks. The black "Warp Sections I–IV" correspond to $\psi_j(\mathbf{x})$ patches; the red "Warp Antisections i–iv" correspond to $\bar{\psi}_\ell(\mathbf{x})$ patches in the boundary expansion of $\Phi|_{\partial\Omega}$.

Criss-cross red paths as exchange currents. The red dashed interlinks in the expanded schematic are encoded by the opposition map $\pi(\ell)$ and the exchange dynamics for $\bar{a}_\ell(t)$, implemented through phase-coupled SFG envelopes (Eq. (18)).

HO and INC as boundary conditions in time and inertia. The HO sets $\theta(t)$ and locks $u_k(t)$ to a coherent phase. The INC enforces $\nabla\Phi \to 0$ near $\mathbf{p}_{\mathrm{INC}}$, which is represented either as a constraint or as a penalty term that flattens gradients.

8. Conclusion

We have formalized the section/antisection warp shell as (i) a PDE-driven warp potential, (ii) a signed decomposition into constructive and counter-curvature domains, (iii) a discrete SFG actuation lattice on the toroidal ring, and (iv) an explicit phase-exchange law coupling opposing antisections through the SFG ring. A closed-loop control topology is provided that is directly consistent with the four schematic depictions and cleanly separates: HO reference, SFG lattice shaping, MEA boundary smoothing, and INC sink constraint.

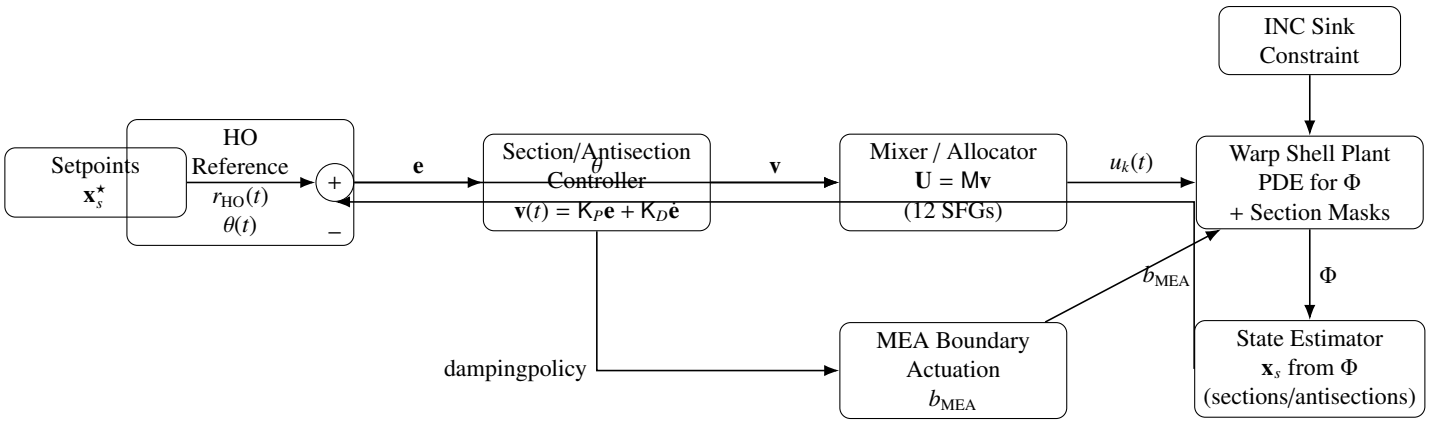

Figure 1: Closed-loop control topology. The HO provides a global phase reference $\theta(t)$ for phase-locked SFG actuation. A section/antisection controller regulates modal amplitudes using estimated shell state. A mixer allocates control effort to the 12 SFGs on the toroidal ring. MEAs supply boundary smoothing/damping. The INC imposes a sink-like constraint that suppresses recoil gradients near the posterior core.